International Journal of Refractory Metals & Hard Materials 72 (2018) 78–82

Contents lists available at ScienceDirect

International Journal of Refractory Metals & Hard Materials

journal homepage: www.elsevier.com/locate/IJRMHM

Fracture toughness of Ti-Si-N thin films

M. Bartosik[a,b,*], R. Hahn[b], Z.L. Zhang[c], I. Ivanov[c], M. Arndt[d], P. Polcik[e], P.H. Mayrhofer[a,b]

[a] Institute of Materials Science and Technology, TU Wien, A-1060 Vienna, Austria
[b] Christian Doppler Laboratory for Application Oriented Coating Development at the Institute of Materials Science and Technology, TU Wien, A-1060 Vienna, Austria
[c] Erich Schmid Institute of Materials Science, Austrian Academy of Sciences, A-8700 Leoben, Austria
[d] Oerlikon Balzers, Oerlikon Surface Solutions AG, LI-9496 Balzers, Liechtenstein
[e] Plansee Composite Materials GmbH, DE-86983 Lechbruck am See, Germany

ARTICLE INFO

Keywords:
TiSiN
Fracture toughness
Micromechanical testing
Single cantilever bending
Damage tolerance

ABSTRACT

Ti-Si-N nanocomposite thin films usually consist of a few nm sized crystals embedded in an amorphous matrix. Here we study the influence of the Si content in Ti-Si-N films – prepared by reactive magnetron sputtering using Ti targets alloyed with intermetallic $TiSi_2$ (to obtain Si contents of 0, 10, 15, 20, 25 at.% in the targets) – on fracture toughness (K_{IC}) and hardness. Single cantilever bending experiments show that Ti-Si-N exhibits K_{IC} values of up to 3.0 ± 0.2 MPa√m, which are significantly higher than those for TiN with 1.9 ± 0.2 MPa√m. Complementary nanoindentation experiments reveal also a higher hardness for Ti-Si-N with 34 ± 1 GPa as compared to 26 ± 1 GPa for TiN. The film structure is carefully studied by X-ray diffraction, X-ray photoelectron spectroscopy, and high-resolution transmission electron microscopy.

1. Introduction

High hardness and toughness in ceramic coatings can be achieved by engineering superlattices [1–4] and (as investigated here) by 3-dimensional nanostructures [5–8], and/or via controlling the electronic structures of the phases. Especially the latter mechanism, which is a material-inherent design, has been demonstrated by a number of authors. For example, Jhi et al. [9] found that a valence-electron concentration (VEC) of 8.4 yields maximum hardness in cubic single-crystal transition metal (TM) nitride and carbide alloys due to σ bonding states between the non-metal p orbitals and the metal d orbitals that strongly resist shearing strain or shape change. As filling of these states is completed at VEC of ~8.4, any additional electrons would go into a higher band which is unstable against shear deformations. Hugosson et al. [10,11] proposed a route for hardness enhancement in TM nitride and carbide alloys by phase stability tuning. For certain VECs different crystal structures have nearly the same total energy. Consequently, at these compositions more than one crystal structure is likely to form. The multiphase/polytypic compounds have a large number of interfaces between structures with different glide systems, which hinder the propagation of dislocations and thereby drastically increase the hardness of the material. Phase stability tuning [12,13] as well as controlling the electronic structure, e.g. by alloying [12,14–16] or vacancies [17], have the potential to not only increase hardness but also toughness of materials.

Coatings with a nano-scale structure are often achieved in heuristic manner. It is not straightforward to predict what synthesis conditions will allow achieving the best properties. On the other hand, the inherent toughness of crystalline phases can be studied and quite well understood *ab initio*, but is often not easily/directly transferrable to practical applications such as industrial coatings.

Titanium-silicon-nitride (Ti-Si-N) coatings exhibit high hardness under optimum deposition conditions that allow complete phase separation and formation of TiN nanocrystals embedded in an amorphous Si_3N_4 matrix phase with a thickness of about one monolayer [18–24]. Oxygen contaminations tend to deteriorate the mechanical properties (see for instance Ref. [25]). The size of the TiN crystals should be only a few nanometer so that neither crystal plasticity (due to dislocations) nor any other form of flaw can develop in the grains [22]. While the hardness of nc-TiN/a-Si_3N_4 nanocomposite coatings has been studied extensively (there are many literature reports like Refs. [5,18–24,26–28].), detailed studies focusing on the fracture toughness of nanocomposite films are yet to be carried out.

The absence of radial cracks after indentation with high loads points towards a high stress threshold for crack initiation in nc-TiN/a-Si_3N_4 coatings. If the nanocrystals are free of flaws, the existence of transgranular cracks is not likely. Hence, initiation and growth of intergranular cracks propagating within the interfacial component should be the most probable fracture mechanism of these materials [22]. Crack deflection within a three-dimensional interfacial network should

* Corresponding author at: Institute of Materials Science and Technology, TU Wien, A-1060 Vienna, Austria.
E-mail address: matthias.bartosik@tuwien.ac.at (M. Bartosik).

https://doi.org/10.1016/j.ijrmhm.2017.12.015
Received 12 October 2017; Received in revised form 14 December 2017; Accepted 15 December 2017
Available online 15 December 2017

further increase the total length of the crack and correspondingly decrease the stress concentration factor [22].

The aim of the present work is to study the fracture toughness (K_{IC}) of Ti-Si-N coatings as a function of Si content. As the fracture toughness is often challenging to quantify using cube corner nanoindentation methods [29], we conducted micro-fracture experiments on free-standing film materials. Single cantilever bending experiments allow to minimize (or even avoid) the influence of residual stresses and substrate interference on the measurements and enable a precise quantification of K_{IC} [30].

2. Experimental

Ti-Si-N coatings with different Si contents were prepared in an AJA Orion 5 lab-scaled magnetron sputter system by DC powering one cathode (power density ~11 W/cm^2) in an Ar/N_2 gas mixture. An Ar/N_2 flow rate ratio of 7/3 and a total pressure of 0.4 Pa were used. For each deposition, the system was equipped with one 3″ Ti target alloyed with intermetallic $TiSi_2$ (Plansee Composite Materials GmbH). The Si contents of the targets were 0, 10, 15, 20, and 25 at.%. To obtain a dense film structure, a bias voltage of − 40 V was applied to the substrates during the deposition process (the floating potential was about − 20 V). Prior to the deposition, the Si (100) substrates (20 × 7 × 0.5 mm^3) were ultrasonically pre-cleaned in acetone and ethanol and mounted on the substrate holder. The substrates were thermally cleaned at 500 °C for 20 min under vacuum conditions and plasma cleaned in a pure Ar atmosphere of a total pressure of 6 Pa for 10 min at the same temperature (by applying a voltage of − 750 V to the substrates). The base pressure in the chamber before the deposition (at room temperature) was below 0.3 mPa. The thickness of the coatings was about 2 µm.

The film chemistry was determined by X-ray photoelectron spectroscopy (XPS) using a SPECS XPS-spectrometer (equipped with Al-K_α radiation).

Structural investigations were performed by X-ray diffraction using a PANalytical X'Pert Pro MPD diffractometer (equipped with Cu-K_α radiation) in symmetric Bragg-Brentano geometry. The coherently diffracting domain size was estimated using the Scherrer formula [31].

The film morphology was studied from fracture cross-sections using a FEI Quanta 200 FEGSEM scanning electron microscope operating with an acceleration voltage of 5 kV.

Further structural characterization was carried out by conventional transmission electron microscopy (TEM) and high resolution (HR)TEM. The microstructure of the TiSiN films was investigated by a JEOL 2100F field emission microscope (200 kV) equipped with an image-side Cs-corrector. Cross-sectional TEM samples were prepared using a standard TEM sample preparation approach. Disks with a diameter of 3 mm diameter were cut out of the material using a cutting machine. The disks were then mechanically thinned and polished to a thickness of about 100 µm, followed by mechanical dimpling until the thinnest part reached a thickness of less than 20 µm. Subsequently, the samples were ion-milled using a Gatan Precision Ion Polishing System until perforation using a voltage of 4 kV and an angle of 4–6°.

The mechanical properties, hardness (H) and Young's modulus (E), were determined by using a Fischer Cripps Laboratories ultra-micro indentation system (UMIS) equipped with a Berkovich tip. At least 29 indents with increasing maximum loads from 3 to 45 mN were carried out for each sample. The data were analyzed using the Oliver and Pharr method [32]. To minimize substrate interference, only indents with indentation depths below 10% of the coating thickness were taken into account.

The fracture toughness of our Ti-Si-N films was determined by micro-fracture experiments performed on free-standing film material. To do so, the Si substrate was chemically etched away using 30% KOH solution at 65 °C for ~1.5 h. From the free-standing film material, µ-beams were FIB machined using a FEI Quanta 200 3D DBFIB work station. The cantilever dimensions were chosen to be ~$t \times t \times 7t$ µm^3, with t being the film thickness, according to the guidelines of Brinckmann et al. [33]. Coarse FIB cuts were made with 1 nA (30 kV), final polishing with 500 pA (30 kV), and the pre-notch with 50 pA (30 kV). The prepared cantilevers were loaded until failure inside a scanning electron microscope (FEI Quanta 200 FEGSEM) by a PI85 PicoIndenter (Hysitron) equipped with a spherical diamond tip (tip radius of ~1 µm), see Fig. 1. The tests were performed displacement-controlled with 5 nm/s. The fracture toughness, K_{IC}, was determined from the maximum load at failure, F_{max}, and the actual cantilever dimensions by applying linear elastic fracture mechanics according to Matoy et al. [34]:

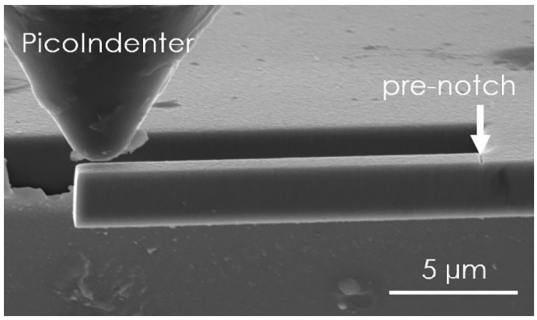

Fig. 1. Scanning electron microscope snap shot showing the PicoIndenter tip as it approaches a pre-notched free-standing Ti-Si-N cantilever. By applying fracture mechanics theory, the fracture toughness, K_{IC}, was determined for our Ti-Si-N coatings from the maximum load at fracture and the actual cantilever and pre-notch dimensions.

$$K_{IC} = \frac{F_{max} \cdot L}{B \cdot W^{3/2}} \cdot f\left(\frac{a}{W}\right) \quad (1)$$

with

$$f\left(\frac{a}{W}\right) = 1.46 + 24.36 \cdot \left(\frac{a}{W}\right) - 47.21 \cdot \left(\frac{a}{W}\right)^2 + 75.18 \cdot \left(\frac{a}{W}\right)^3. \quad (2)$$

Here, L denotes the distance between pre-notch and the point of applied force, B the width of the cantilever, W the thickness of the cantilever. The pre-notch crack length, a, was measured from scanning electron micrographs of the post mortem fracture cross-sections. The length of the pre-notch was in the order of 0.1 to 0.18t. Overall, 25 samples were tested (5 for each coating composition) with an average success rate of over 80%.

3. Results and discussions

X-ray photoelectron spectroscopy analyses (not shown) suggest Si contents of 0, 5.0, 8.5, 10.5, and 13.8 at.% in the coatings (the Si contents of the targets were: 0, 10, 15, 20, and 25 at.%), indicating that almost stoichiometric nitrides are formed. The Si 2p feature seen in the XPS signals corresponding to Si fourfold coordinated to nitrogen suggests that Si in our Ti-Si-N coatings is bonded as in Si_3N_4.

X-ray diffraction patterns of our Ti-Si-N films, presented in Fig. 2, show that the only crystalline phase can best be described by face-centered cubic TiN with (111) preferred crystallographic orientation (especially for higher Si contents). Our data actually suggest highly distorted TiN lattices for coatings containing 5 to 10.5 at.% Si, as the (111) XRD peak is shifted to the right from the standard position of TiN but the (200) XRD peak is close to the standard position of TiN. This would correspond to a tetragonally distorted cubic lattice. Hence, the c-axis is significantly smaller than the lattice parameter of TiN. Smaller lattice parameters of Si-alloyed TiN have already been observed earlier experimentally [35] and theoretically [36,37]. The increase in peak broadening with increasing Si content suggests reduced crystallite sizes. A rough estimation of the coherently diffracting domain size using the Scherrer formula — neglecting the contribution of microstrains to the